

Bounds on the yield stress of cohesionless granular matter

Wouter G. Ellenbroek¹ and Jacco H. Snoeijer²

¹*Instituut–Lorentz, Universiteit Leiden, Postbus 9506, 2300 RA Leiden, The Netherlands*

²*School of Mathematics, University of Bristol, University Walk, Bristol BS8 1TW, United Kingdom*

(Dated: December 2, 2024)

We characterize the force state of shear-loaded granular matter by relating the macroscopic stress to statistical properties of the force network. It is demonstrated how force anisotropies naturally provide an upper bound for the shear stress. We establish a relation between the maximum possible shear resistance and the friction coefficient between individual grains, and find that anisotropies of the contact network (or the fabric tensor) only have a subdominant effect. Finally, we discuss how force anisotropies can be related quantitatively to experimental measurements of the effective elastic constants.

PACS numbers: 45.70.Cc, 05.40.-a, 46.65.+g

I. INTRODUCTION

An assembly of cohesionless granular matter, in which there is no attraction between grains, can only exist when held together by an external pressure [1]. The distribution of these confining forces throughout the material is a complex process that involves a highly inhomogeneous network of contact forces [2, 3, 4, 5]. Force networks as shown in Fig. 1a are typical for a broad variety of amorphous systems like foams, colloids and emulsions, and play a crucial role for understanding the macroscopic mechanical properties [6, 7, 8].

A robust feature of these “jammed” materials is that they can sustain a certain amount of shear stress before failure [9, 10, 11, 12]. There are many aspects that influence this shear resistance or internal friction of a granular material. A well known example is that wet sand can sustain much larger shear stresses than dry sand, due to the presence of attractive liquid bridges [13, 14]. The strength of the assembly is also enhanced by increasing intergrain friction or roughness of the grains. Less obvious are effects related to the geometry of the particle packing, that involve fabric anisotropy or coordination number of the material [15, 16, 17, 18]. It was recently found for frictionless systems that packings close to the minimum isostatic coordination number can hardly support any stress [19], whereas strongly hyperstatic packings sustain much more [20]. It has remained a great challenge to understand how these phenomena are related to the strongly anisotropic force networks.

In this paper we derive analytical upper bounds for the yield stress of cohesionless granular media, for varying intergrain friction and fabric anisotropy. We describe the force anisotropies using *averages* of interparticle forces, denoted $\bar{\mathbf{f}}(\phi)$, as a function of the orientation ϕ of the contact – see Fig. 1b. This object has recently been accessed experimentally for the first time [8], and contains much more information than the stress tensor: the stress is basically a projection of $\bar{\mathbf{f}}(\phi)$ [20, 21, 22]. A crucial observation is that one can directly translate the physical constraints for all individual contact forces, namely

- normal forces are purely repulsive, i.e. $f_n \geq 0$,

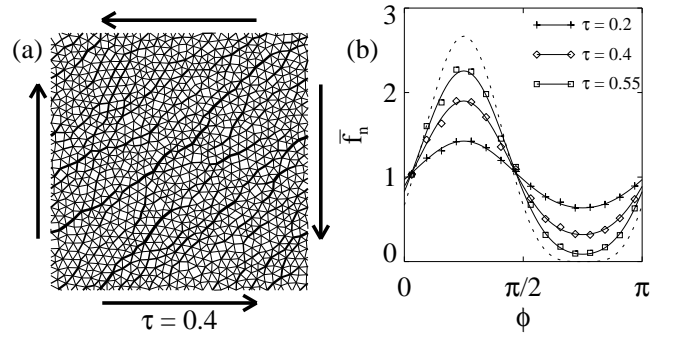


FIG. 1: (a) Force network obtained from a numerical simulation of a strongly hyperstatic frictionless granular material (coordination number $z = 5.75$) subjected to a shear stress $\tau = \sigma_{xy}/\sigma_{xx}$, using the “force network ensemble” [5, 20]. The thicknesses of lines represent the strength of the forces. (b) Corresponding average contact force as a function of contact angle ϕ for this ensemble of force networks. Increasing the shear stress yields a modulation of $\bar{f}(\phi)$ that is accurately described by the form $1 + 2\tau \sin 2\phi + b_2 \cos 4\phi$. For large stress, $\bar{f}(\phi)$ approaches the limiting curve predicted by Eq. (19).

- tangential forces f_t obey Coulomb’s law of friction, $|f_t| \leq \mu f_n$,

to constraints for their averaged values $\bar{\mathbf{f}}(\phi)$. Here, μ is the Coulomb friction coefficient of the individual contacts. We show how one can obtain nontrivial predictions for the yield stress of granular media by finding the extreme forms of $\bar{\mathbf{f}}(\phi)$. While these bounds can probably not be reached in real systems, they provide a well-defined analytical tool to investigate the influence of the micromechanical parameters on the effective macroscopic friction. Furthermore, we demonstrate that $\bar{\mathbf{f}}(\phi)$ can be used to obtain a mean-field prediction for the effective elastic coefficients of the material, which were recently found to be highly anisotropic in response experiments [6, 23].

The relevant macroscopic quantity is the deviatoric stress, defined as $\tau = (\sigma_1 - \sigma_2)/(\sigma_1 + \sigma_2)$, where the σ_i denote the principal values of the stress tensor. We work in the coordinate frame where $\sigma_{xx} = \sigma_{yy}$, so we

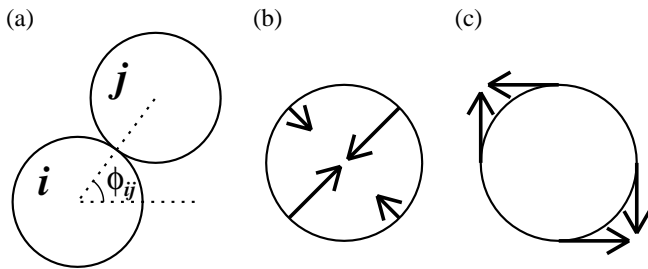


FIG. 2: (a) Definition of contact orientation ϕ_{ij} . (b,c) Illustration of the (average) bias of normal and tangential forces onto a particle due to the imposed shear stress.

can express the deviatoric stress as $\tau = \sigma_{xy}/\sigma_{xx}$. For cohesionless systems one may naively expect that the ultimate shear stress is achieved when one principal direction becomes tensile, e.g. $\sigma_2 = 0$, which would lead to $\tau_{\max} = 1$. By invoking realistic structures of $\mathbf{f}(\phi)$ for granular packs, however, we show that the physics is in fact much more subtle. Our main findings are: (i) the real bound is typically much lower than unity due to steric exclusion of neighboring grains; (ii) the effect of friction between grains is surprisingly mild: a typical Coulomb friction coefficient of $\mu = 0.5$ increases τ_{\max} by only 16% as compared to the frictionless case. (iii) realistic anisotropies in the contact fabric hardly increase τ_{\max} and thus play a subdominant role.

The approach followed in the paper basically forms a worst-case analysis, in which we optimize the form of $\mathbf{f}(\phi)$ in order to resist the highest possible value of τ . We do not take into account the conditions imposed by mechanical equilibrium on all grains in the system. It is clear that our description is not very realistic for packings near the isostatic limit [24, 25], for which the forces are entirely determined by the constraints of force balance. These systems are extremely fragile and have a vanishing shear resistance [19]. For strongly hyperstatic systems (i.e. high coordination numbers), however, the mechanical equilibrium conditions become much less restrictive and still allow for a multitude of different force solutions. We have recently performed a detailed numerical study for a broad range of coordination numbers, exploring this “ensemble of force networks” [5, 26, 27] that explicitly respect force balance. Our numerical results clearly show that the upper bounds *do* provide realistic predictions for packings that are strongly hyperstatic [20]. Such packings have a lot of available force balance solutions and are thus more likely to reach the extreme shapes of $\mathbf{f}(\phi)$ predicted by our analysis. The present work provides a full exposition and generalization of the arguments put forward in Ref. [20].

The paper is organized as follows. We first define the quantities that will be used to analyse the bounds, defined from the microscopic structure of grains and contacts, in relation to the macroscopic shear stress in Sec. II. The third section addresses the simplest case of isotropic, frictionless packings, and shows how the gran-

ularity of the material affects the maximally supportable shear stress. In Secs. IV and V we explore the effects of intergrain friction and fabric anisotropies on the bounds. We conclude in Sec. VI, where we argue how our approach can be applied to problems of anisotropic elasticity.

II. FROM CONTACT FORCES TO MACROSCOPIC STRESS

We consider two-dimensional packings of discs, so that the orientations of the contacts between particles *i* and *j* can be characterized by the angle (Fig. 2a)

$$\phi_{ij} = \arccos \left(\frac{x_j - x_i}{|\mathbf{r}_j - \mathbf{r}_i|} \right). \quad (1)$$

Here \mathbf{r}_i denotes the position vector of particle *i* and x_i its *x*-coordinate. The key quantity that we will use to determine bounds on the yield stress is the average force $\bar{\mathbf{f}}(\phi)$ carried by all contacts of orientation ϕ . Since bond directions have no polarity, the angle only assumes values $0 \leq \phi < \pi$, and the period of $\bar{\mathbf{f}}(\phi)$ is π . One can relate $\bar{\mathbf{f}}(\phi)$ to the stress tensor σ , using [21]

$$\sigma_{\alpha\beta} = \frac{1}{V} \sum_{\{ij\}} (\mathbf{f}_{ij})_{\alpha} (\mathbf{r}_{ij})_{\beta} \equiv \frac{N_c}{V} \overline{\mathbf{f}_{\alpha} \mathbf{r}_{\beta}}. \quad (2)$$

Here α, β label coordinate axes, N_c is the number of contacts in the (two-dimensional) volume *V*, $\mathbf{r}_{ij} = \mathbf{r}_j - \mathbf{r}_i$, and \mathbf{f}_{ij} is the force exerted on particle *j* by particle *i*. The bar indicates average over all forces in *V*. We decompose the force vector in a normal component, $f_{n,ij}$, and tangential components, $f_{t,ij}$, as

$$(\mathbf{f}_{ij})_x = f_{n,ij} \cos \phi_{ij} - f_{t,ij} \sin \phi_{ij} \quad (3)$$

$$(\mathbf{f}_{ij})_y = f_{n,ij} \sin \phi_{ij} + f_{t,ij} \cos \phi_{ij}. \quad (4)$$

The sign conventions are such that repulsive forces have positive $f_{n,ij}$, while the tangential component is positive when pointing “counterclockwise” with respect to particle *i* (see Fig. 2).

For large enough packings we can express the stress tensor in a statistical form, evaluating the average $\overline{\mathbf{f}_{\alpha} \mathbf{r}_{\beta}}$ from the probability to find a contact with force \mathbf{f}_{ij} and center-to-center vector \mathbf{r}_{ij} . In terms of normal and tangential components, and with the observation that the forces are uncorrelated to the interparticle distance $|\mathbf{r}_{ij}|$ [20, 22], this involves the joint probability $P(f_n, f_t, \phi)$. We can explicitly factorize the contact angle probability $\Phi(\phi)$ to write

$$P(f_n, f_t, \phi) = \Phi(\phi) P_{\phi}(f_n, f_t).$$

The distribution $P_{\phi}(f_n, f_t)$ has been introduced recently [20] and is properly normalized to unity. Hence, the probabilistic form of the stress tensor reads

$$\begin{aligned}
\sigma_{\alpha\beta} &= \frac{\bar{r}N_c}{V} \int_0^\pi d\phi \Phi(\phi) \int_0^\infty df_n \int_{-\infty}^\infty df_t \\
&\quad \times P_\phi(f_n, f_t) [f_n \mathcal{N}_{\alpha\beta} + f_t \mathcal{T}_{\alpha\beta}] \\
&= \frac{\bar{r}N_c}{V} \int_0^\pi d\phi \Phi(\phi) [\bar{f}_n(\phi) \mathcal{N}_{\alpha\beta} + \bar{f}_t(\phi) \mathcal{T}_{\alpha\beta}], \quad (5)
\end{aligned}$$

where \bar{r} denotes the average interparticle distance. The projection factors have been collected in tensors $\mathcal{N}_{\alpha\beta}$ and $\mathcal{T}_{\alpha\beta}$, written in matrix notation as

$$\mathcal{N}_{\alpha\beta} = \begin{pmatrix} \cos^2 \phi & \cos \phi \sin \phi \\ \cos \phi \sin \phi & \sin^2 \phi \end{pmatrix} \quad (6)$$

$$\mathcal{T}_{\alpha\beta} = \begin{pmatrix} -\cos \phi \sin \phi & -\sin^2 \phi \\ \cos^2 \phi & \cos \phi \sin \phi \end{pmatrix}. \quad (7)$$

In the remainder, we will set the prefactor $\bar{r}N_c/V = 1$ in Eq. (5).

The above analysis allows computing the stress from $\bar{\mathbf{f}}(\phi)$. To relate the force anisotropies to the shear stress, a common trick is to expand $\bar{\mathbf{f}}(\phi)$ in a Fourier series [16, 20, 22]

$$\bar{f}_n(\phi) = \sum_{k=1}^N a_k \sin 2k\phi + \sum_{k=0}^N b_k \cos 2k\phi \quad (8)$$

$$\bar{f}_t(\phi) = \sum_{k=1}^N c_k \sin 2k\phi + \sum_{k=0}^N d_k \cos 2k\phi. \quad (9)$$

Because we are working in the frame where $\sigma_{xx} = \sigma_{yy}$, the principal axes of stress point in the directions (1, 1) and (1, -1). These directions must then be lines of mirror symmetry, as is illustrated in Fig. 2, which makes that $a_k = d_k = 0$ for even k and $b_k = c_k = 0$ for odd k .

For the moment, until the last section of the paper, we will consider the case where the fabric is isotropic so $\Phi(\phi) = 1/\pi$. In that case, inserting Eqs. (8,9) in Eq. (5) and integrating yields

$$\sigma_{xx} = b_0/2 \quad (10)$$

$$\sigma_{yy} = b_0/2 \quad (11)$$

$$\sigma_{xy} = (a_1 + d_1)/4. \quad (12)$$

All higher order terms in the expansion yield zero upon integration. Our main interest is the deviatoric stress, so we are free to choose the pressure scale as $\sigma_{xx} = \sigma_{yy} = 1/2$, so that $\bar{f} = b_0 = 1$ and

$$\tau = \frac{a_1 + d_1}{2}. \quad (13)$$

This relation reveals how an applied shear stress can be sustained through anisotropies in both the normal and frictional forces, via a_1 and d_1 respectively [22]. The strategy will be to explore the physical limitations of a_1 and d_1 , which will provide a bound on τ .

III. FRICTIONLESS PACKINGS

We start out with packings of frictionless particles, for which the problem of the maximum possible deviatoric stress is relatively straightforward. In this case a bound on τ emerges from the purely repulsive nature of the forces: all contacts have $f_{n,ij} \geq 0$, so certainly the averages should obey

$$\bar{f}_n(\phi) \geq 0, \quad (14)$$

for all values of ϕ . This condition obviously forms a serious restriction on the amplitude of the force anisotropy, and we show how this yields an upper limit on τ . We show that this maximum value τ_{\max} depends on the number of terms included in the Fourier series of Eq. (8): even though the higher order terms do not contribute to the stress, they enable $f_{n,ij}$ to reach more extreme shapes. Supported by existing numerical results [20] however, we argue that steric exclusion between neighboring grains will in practice cut off the series beyond $k = 2$.

A. Realistic $\bar{f}_n(\phi)$

For the frictionless case we have from Eq. (13)

$$a_1 = 2\tau, \quad d_1 = 0, \quad (15)$$

so that Eq. (8) becomes

$$\bar{f}_n(\phi) = 1 + 2\tau \sin 2\phi + b_2 \cos 4\phi + \dots \quad (16)$$

Let us first consider the simplest case, in which we truncate after the lowest anisotropic term, i.e. $\bar{f}_n(\phi) = 1 + 2\tau \sin 2\phi$, so that τ is the only free parameter. For positive τ this function has a minimum in $\phi = 3\pi/4$, which touches $\bar{f}_n(\phi) = 0$ for $2\tau = 1$. Hence, $\tau_{\max} = 1/2$. In the same way we could derive $\tau_{\min} = -1/2$. From now on we will only consider positive τ , without loss of generality.

From the numerical result of Fig. 1b it is clear that the modulation does not stay symmetric around $\bar{f}_n(\phi) = 1$ for large values of τ . This indicates a significant contribution of the type $\cos 4\phi$. In fact, this is the highest order term that is observed in numerical simulations [20].

We thus focus on the case $N = 2$ in the expansion (8). The optimization problem involves two free parameters, τ and b_2 . We are free to vary b_2 in such a way as to facilitate a maximum τ , under the constraint that $\bar{f}_n(\phi) \geq 0$ for all ϕ . We furthermore demand that $\bar{f}_n(\phi)$ evolves monotonically between the principal directions at $\phi = \pi/4$ and $\phi = 3\pi/4$. This implies that the minimum of $\bar{f}_n(\phi)$ should stay at $\phi = 3\pi/4$, as it is the case in the numerics of Fig. 1b. Physically, this means that the first contacts to break are those oriented in the direction in which the material is stretched. While the expansion ensures that there is an extremum in $\phi = 3\pi/4$, this extremum only

remains a minimum if

$$\left. \frac{\partial^2}{\partial \phi^2} \bar{f}_n(\phi) \right|_{\phi=3\pi/4} = 8\tau + 16b_2 \geq 0 .$$

The value of $\bar{f}_n(\phi)$ in this minimum must satisfy

$$\bar{f}_n(3\pi/4) = 1 - 2\tau - b_2 \geq 0 .$$

This defines a linear program with parameters τ and b_2 , two inequalities, and the objective to maximize τ . The solution is easily found to be [28]

$$\tau_{\max} = \frac{2}{3} \quad (17)$$

$$b_2 = -\frac{1}{3} . \quad (18)$$

Fig. 1b illustrates the relevance of this bound for strongly hyperstatic packings: the numerical $\bar{f}_n(\phi)$ (taken from [20]) indeed approaches the limiting form (dashed curve)

$$\bar{f}_n(\phi) = 1 + \frac{2}{3} \sin 2\phi - \frac{1}{3} \cos 4\phi . \quad (19)$$

So indeed, the system is able to organize the forces in such a manner as to optimize the sustained shear stress.

1. Steric exclusion and the width of $\bar{f}_n(\phi)$

Let us argue how the finite width of $\bar{f}_n(\phi)$, which allowed to truncate the Fourier series at $N = 2$, is due to steric exclusion between neighboring grains. Suppose we know that a given grain has a contact in direction ϕ_{ij} . Then, because all grains occupy some space, there can be no other contacts at directions in roughly the interval $[\phi_{ij} - \pi/3, \phi_{ij} + \pi/3]$. These very local correlations have been shown to be important for several aspects of granular packings [29, 30]. For example it leads to a bound on the fabric anisotropy [29] (see also Sec. V). For our purpose the main effect is that for a grain i , the strongest contact $f_{\max,i}$ is scattered around the major stress axis within a range of $\pi/3$. Because the forces on each grain balance, there is a finite fraction of grains j for which $f_{\max,j}$ is of the same order as $f_{\max,i}$. The isotropic contact network then ensures a broad $\bar{f}_n(\phi)$, with a width of about $\pi/3$. Therefore, the Fourier expansion with $N = 2$ provides an excellent description – see e.g. Ref. [20] for detailed comparison with numerics.

B. The limit $N \rightarrow \infty$ and tensile stresses

Although Fourier terms with $k \geq 3$ do not play a role in granular systems, it is insightful to study the general case where we truncate the series at arbitrary order N . The expansion now contains N free coefficients that we need to fix, in order to optimize τ . In the case $N = 2$, we

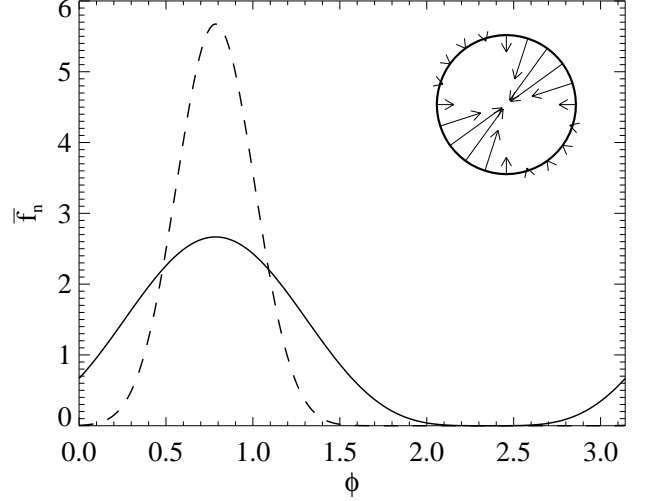


FIG. 3: The optimized $\bar{f}_n(\phi)$ for $N = 2$ (solid), $N = 10$ (dashed). The figure in the corner illustrates the corresponding average force exerted on a particle for various contact orientations ($N = 2$).

invoked the condition $\partial^2 \bar{f}_n / \partial \phi^2 \geq 0$ at $\phi = 3\pi/4$ to ensure that the minor principal axis remains a minimum of $\bar{f}_n(\phi)$, and taking $\partial^2 \bar{f}_n / \partial \phi^2 = 0$ turned out to maximize τ . A nonzero $k = 3$ term allows to also fix $\partial^4 \bar{f}_n / \partial \phi^4$ in such a way that τ becomes even larger. The upshot of adding more terms is that we can make $\bar{f}_n(\phi)$ as flat (and as close to zero) as possible around $\phi = 3\pi/4$, where the contribution to the overlap with $\sin 2\phi$ is negative. Every time we have to verify that the first nonzero Taylor coefficient when expanding around $\phi = 3\pi/4$ is positive, so that we are indeed dealing with a minimum.

The general scheme is thus that adding the term of order k generates an additional condition that $\partial^{(2k-2)} \bar{f}_n / \partial \phi^{(2k-2)} = 0$. For general N , this yields the following set of linear equations:

$$\left. \frac{\partial^{2l}}{\partial \phi^{2l}} \bar{f}_n(\phi) \right|_{\phi=3\pi/4} = 0 \quad \text{for all } l = 0, 2, \dots, N-1 . \quad (20)$$

In App. A we show that this linear problem for the Fourier coefficients can be inverted analytically, yielding a remarkably simple result for the maximum τ , namely

$$\tau_{\max}(N) = \frac{N}{N+1} . \quad (21)$$

Interestingly, this reveals an ultimate (mathematical) upper bound $\tau_{\max} = 1$. We plotted the optimized $\bar{f}_n(\phi)$ for various values of N (Fig. 3): clearly, $\bar{f}_n(\phi)$ evolves towards the extreme case of a Dirac δ -peak in the limit $N \rightarrow \infty$. As already mentioned in the introduction, this condition of $\tau = 1$ precisely corresponds to the point where the minor principal axis becomes tensile. We thus conclude that the maximum stress for a frictionless packing lies well below the point where the global stress develops a tensile direction, due to the finite width of $\bar{f}_n(\phi)$.

This illustrates how correlations due to steric exclusion, discussed in Sec. III A, can play an important role for the overall mechanical properties.

IV. FRICTIONAL PACKINGS: $\tau(\mu)$

The presence of frictional forces provides an additional degree of freedom to develop anisotropic stresses: Eq. (13) shows that the total deviatoric is the sum of the (lowest order) anisotropies of normal and tangential forces. It is clear that this will enhance the ability to sustain a large external load. However, there is again a bound on the force anisotropies, now due to Coulomb's law for individual contacts, i.e. $|f_{t,ij}| \leq \mu f_{n,ij}$, where μ is the microscopic Coulomb friction coefficient. Since this condition should hold for any pair of grains, it certainly holds for the averages:

$$|\bar{f}_t(\phi)| \leq \mu \bar{f}_n(\phi) . \quad (22)$$

This condition is illustrated in Fig. 4. In this section we derive how τ_{\max} depends on the value of μ , again using the Fourier expansions of $\bar{f}_n(\phi)$ and $\bar{f}_t(\phi)$ up to $N = 2$.

A. The optimization problem

From Eq. (13) we can express

$$a_1 = 2\tau - d_1 , \quad (23)$$

so that

$$\bar{f}_n(\phi) = 1 + (2\tau - d_1) \sin 2\phi + b_2 \cos 4\phi , \quad (24)$$

$$\bar{f}_t(\phi) = d_1 \cos 2\phi + c_2 \sin 4\phi . \quad (25)$$

Let us now take a value of τ slightly above the frictionless limit $2/3$. The prefactor in front of the $\sin 2\phi$ term can now be lowered due to d_1 , i.e. due to the presence of friction. If we put τ far above $2/3$, however, one requires a relatively large d_1 . The value of d_1 is bounded by the condition of Eq. (22), so that not all τ can be reached.

To determine the maximum value of τ as a function of μ , we have to specify acceptable values of the higher order coefficients b_2 and c_2 , which do not contribute to the stress tensor. As we did in the frictionless case, we demand that the function $\bar{f}_n(\phi)$ evolves monotonically between major and minor directions, so that it has only one maximum (in the major direction) and only one minimum (in the minor direction). A similar requirement is imposed on $\bar{f}_t(\phi)$: the average tangential force only changes sign along the principal directions, see e.g. Fig. 4. If this were not the case, the tangential forces would swap from clockwise to counterclockwise and back in between the major and minor directions. Such a spontaneous symmetry breaking would introduce a very non-generic organization of forces within the packing. These

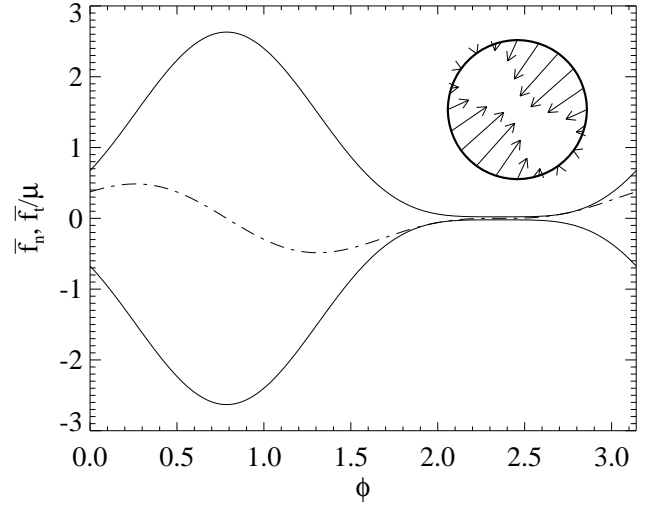


FIG. 4: The frictional optimization problem for $\mu = 0.28$. The solid lines represent $\pm \bar{f}_n(\phi)$, the dash-dotted line $\bar{f}_t(\phi)/\mu$, which has to satisfy Eq. (22). The figure in the corner illustrates the average force exerted on a frictional particle for various contact orientations. Note that these forces now have tangential components.

conditions put bounds on the second order coefficients,

$$-\frac{2\tau - d_1}{4} \leq b_2 \leq \frac{2\tau - d_1}{4} , \quad (26)$$

$$-\frac{d_1}{2} \leq c_2 \leq \frac{d_1}{2} . \quad (27)$$

We have numerically solved this optimization problem by varying all possible values of the parameters τ, d_1, b_2, c_2 , within the ranges imposed by Eqs. (22,26,27). The results are shown in Fig. 5. Surprisingly, the dependence on μ is relatively weak. In the paragraph below we obtain the analytical result,

$$\tau_{\max} = \frac{1 + \sqrt{1 + 3\mu^2}}{3} ,$$

which is derived for $0.29 \lesssim \mu \leq 1$. However, Fig. 5 shows that this is a very good approximation outside this range as well.

B. Analytical solution of $\tau(\mu)$

The set of parameters τ, d_1, b_2, c_2 that corresponds to the maximum value of τ obviously corresponds to functions $\bar{f}_t(\phi)$ and $\mu \bar{f}_n(\phi)$ that are tangent in at least one point. We will now derive the optimal set of parameters for the case there is a tangent point in the interval $\frac{7\pi}{8} \leq \phi \leq \pi$, and then determine for what range of μ this is the case.

In the interval $[\frac{7\pi}{8}, \pi]$, the $\cos 2\phi$ in $\bar{f}_t(\phi)$ is positive and the $\sin 4\phi$ is negative. We want to have a d_1 which is large (to facilitate larger τ), and at the same time a

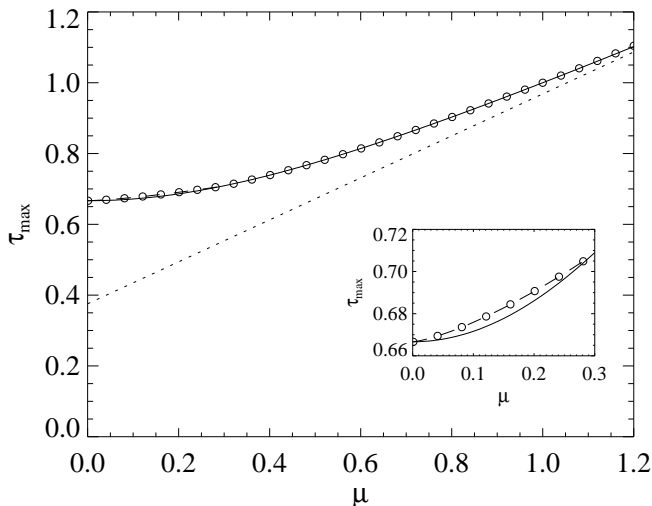


FIG. 5: The optimized $\tau(\mu)$ for frictional packings with isotropic fabric. The circles are numerical data. The solid line is Eq. (28). The dashed line is the analytic result for $\mu \lesssim 0.29$. The dotted line is the asymptote $\tau \propto 0.593\mu$ as $\mu \rightarrow \infty$. The inset shows an enlargement of the small μ region.

$\bar{f}_t(\phi)$ which is as close to zero as possible (to stay away from violating Eq. (22)). Therefore, the parameter c_2 should have its maximum value $c_2 = d_1/2$, as dictated by Eq. (27). Similarly, we want $\bar{f}_n(\phi)$ to be as large as possible, and hence because $\cos 4\phi$ is positive in the considered interval, b_2 should also be maximal. There are two upper bounds on b_2 , given by Eq. (26) and $\bar{f}_n(\phi) \geq 0$, the latter of which turns out to be the most restrictive one. This gives

$$b_2 = 1 + d_1 - 2\tau.$$

Having eliminated b_2 and c_2 , we have thus reduced the optimization problem to 2 parameters, namely τ and d_1 . To find the parameters that maximize τ , we take the equality sign in Eq. (22) and demand that solutions are tangent points. For arbitrary values of the parameters, there is a tangent point in $\phi_1 = 3\pi/4$ and two normal intersection points in ϕ_2 and ϕ_3 . The intersection points should coincide to turn into a tangent point. Equating $\phi_2 = \phi_3$ gives a relation between the parameters which, after some lengthy but elementary algebra, can be written as

$$\tau = \frac{1}{2}d_1 + \frac{1}{3} + \frac{1}{6\mu}\sqrt{4\mu^2 - 3d_1^2}.$$

Maximizing this expression for $\tau(\mu, d_1)$ with respect to d_1 yields that the optimum is obtained for

$$d_1 = \frac{2\mu^2}{\sqrt{1 + 3\mu^2}},$$

so that

$$\tau_{\max}(\mu) = \frac{1 + \sqrt{1 + 3\mu^2}}{3}. \quad (28)$$

Inserting these into the original equations gives the value of ϕ where the curves touch,

$$\tan 2\phi = \frac{\sqrt{1 + 3\mu^2} - 2}{3\mu}, \quad (29)$$

which was demanded to be in the interval $[\frac{7\pi}{8}, \pi]$. This requirement is met for values of μ satisfying

$$(0.29 \approx) 1 - \frac{1}{2}\sqrt{2} \leq \mu \leq 1. \quad (30)$$

This validity is indeed found numerically in Fig. 5. Note that this range of Coulomb coefficients is the most relevant for real granular materials [31].

For smaller μ the tangent point is below $\phi = \frac{7\pi}{8}$, where the $\cos 4\phi$ is negative, so b_2 should now be as small as possible: $b_2 = -(2\tau - d)/4$. The resulting quartic equations can be solved using computer algebra, yielding a lengthy expression (not shown), which is plotted as the dashed part of the curve in Fig. 5, and which coincides with the numerical data.

For $\mu > 1$ the above analysis gives a tangent point in the interval $[0, \pi/12]$, so that the considerations that allowed us to fix b_2 and c_2 are no longer valid and we only have the numerical result of Fig. 5. When the Coulomb coefficient becomes very large, the sustainable shear stress is mostly due to the tangential forces. Because the right hand side of Eq. (22) grows linearly with μ , the values of d_1 and c_2 can also scale as μ when $\mu \gg 1$. This leads to an asymptotic behavior of $\tau_{\max}(\mu)$ which is linear in μ . We numerically determined the parameters $a_1, b_2, c_2/\mu, d_1/\mu$ for the asymptotic $\bar{f}_n(\phi)$ and $\bar{f}_t(\phi)/\mu$ by optimizing for d_1/μ instead of τ . The resulting asymptote is $\tau = 0.376 + 0.593\mu$, which plotted as the dotted line in Fig. 5.

V. FABRIC ANISOTROPY

We now analyze the effect of a fabric anisotropy on the yield stress bounds. The structure of the contact network can be characterized using the fabric tensor $F_{\alpha\beta} = \mathbf{r}_\alpha \mathbf{r}_\beta / r^2$, and a fabric anisotropy shows up as a difference between the principal values of this tensor, $F_1 - F_2$. Analogous to the stress tensor, this difference is solely determined by the lowest order coefficient of the Fourier expansion of $\Phi(\phi)$, the contact angle distribution, which we therefore approximate as [32]

$$\Phi(\phi) = \frac{1}{\pi}(1 + p_1 \sin 2\phi). \quad (31)$$

One easily shows that $p_1 = 2(F_1 - F_2)$. The strategy is to again find the maximum possible value for τ , but now for $p_1 \neq 0$.

Let us note that this truncated form for $\Phi(\phi)$ is a good approximation for systems with a simple shear deformation history [22, 33], although more complex forms are encountered e.g. for packings formed under gravity [34].

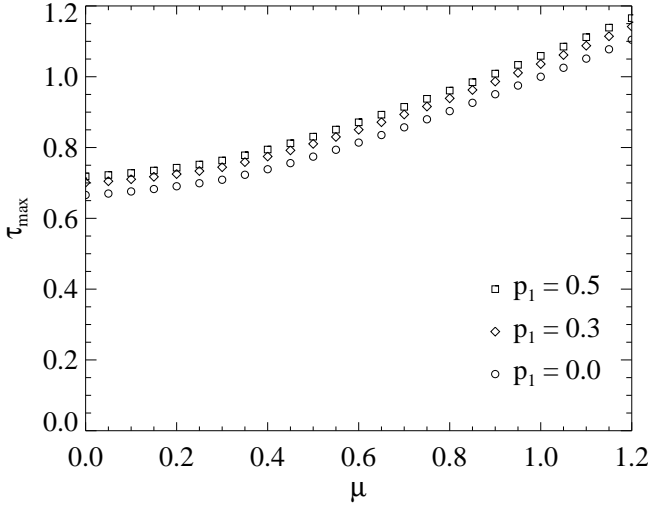


FIG. 6: Maximum shear stress τ_{\max} as a function of friction coefficient μ for $p_1 = 0, 0.3, 0.5$.

As was demonstrated by Troadec *et al.* [29], the values for p_1 are bounded by the effect of steric exclusion between neighboring contacts (see also Sec. III A 1). Indeed, numerical simulations show that $p_1 < 0.3$, while typically p_1 is of the order 0.1 [22, 33].

We thus insert the form Eq. (31) in the expression for the stress tensor Eq. (5), yielding

$$\sigma_{xx} = b_0/2 + p_1 a_1/4 \quad (32)$$

$$\sigma_{yy} = b_0/2 + p_1 a_1/4 \quad (33)$$

$$\sigma_{xy} = \frac{1}{4}(a_1 + d_1) + \frac{p_1}{8}(2b_0 + c_2 - b_2). \quad (34)$$

This time the second order coefficients *do* affect the value of the deviatoric stress directly. The idea of the optimization procedure, however, remains the same as in the isotropic case. We will first work out the frictionless case analytically, and then present numerical results for frictional particles.

A. Anisotropic frictionless systems

Without friction, $c_2 = d_1 = 0$, and from Eqs. (32,34) the deviatoric stress now reads

$$\tau = \frac{\sigma_{xy}}{\sigma_{xx}} = \frac{2a_1 + 2p_1 b_0 - p_1 b_2}{2p_1 a_1 + 4b_0}.$$

We will again fix the pressure scale as $\sigma_{xx} = \sigma_{yy} = 1/2$, so that we can eliminate b_0 :

$$b_0 = 1 - \frac{p_1 a_1}{2} \quad (35)$$

$$\tau = \frac{a_1(2 - p_1^2) + p_1(2 - b_2)}{4}. \quad (36)$$

The physical constraints on a_1 and b_2 are the same as for the isotropic case discussed in Sec. III A, but the optimization target is now given by Eq. (36), instead of

the $\tau = a_1/2$ we had before. The constraints follow from $\bar{f}_n(\phi)$ and its second derivative being nonnegative at $\phi = 3\pi/4$:

$$b_2 \leq 1 - a_1(1 + p_1/2) \quad (37)$$

$$b_2 \geq -a_1/4. \quad (38)$$

The solution to this linear program is then found to be

$$a_1 = 4/(2p_1 + 3) \quad (39)$$

$$b_0 = 3/(2p_1 + 3) \quad (40)$$

$$b_2 = -1/(2p_1 + 3), \quad (41)$$

which corresponds to

$$\tau_{\max} = \frac{7p_1 + 8}{8p_1 + 12}. \quad (42)$$

The inclusion of fabric anisotropy hence leads to a small increase of the maximum deviatoric stress; for e.g. $p_1 = 0.3$ we get a 5% increase. See also the numerical data points on the vertical axis of Fig. 6.

B. Anisotropic systems with friction

Now let us discuss the complete case, with anisotropic fabric and finite friction coefficient. Because σ_{xx} does not involve the tangential forces, b_0 is still given by Eq.(35). The deviatoric is now found from Eq. (34) to be

$$\tau = \frac{a_1(2 - p_1^2) + 2d_1 + p_1(2 - b_2 + c_2)}{4}. \quad (43)$$

This has to be maximized with the constraint of the averaged Coulomb condition Eq. (22). For this problem, we have used the same numerical optimization as in Sec. IV A. The result is shown for $p_1 = 0.3, 0.5$ in Fig. 6. From this figure one can see that the combined effect of friction and anisotropy can roughly be seen as an addition of their individual effects.

VI. DISCUSSION

We have derived upper bounds for the yield stress of static granular materials, τ_{\max} , by finding the extreme shapes of the angle-resolved average force, $\bar{\mathbf{f}}(\phi)$, that are consistent with Coulomb's friction law for individual grains. While these extreme states can probably not be reached in real systems, they provide a well-defined analytical tool to investigate the influence of the micromechanical parameters on the effective macroscopic friction. Our results are most relevant for strongly hyperstatic systems, since these have more "freedom" in their force networks to accommodate the shear stress [20].

A first result is that the effect of fabric anisotropy is relatively weak and only mildly enhances the shear resistance of an assembly. This suggests that shear-induced

textures observed in numerical simulations [22, 33] play a relatively passive role in the stress balance.

We also computed the maximum stress as a function of the microscopic friction coefficient μ . Surprisingly, τ_{\max} does not increase rapidly with μ (Fig. 5). Such a weak dependence is consistent with internal friction measured in simulations of quasi-static shear flows [16], where a mild increase is observed when $\mu > 0.4$. In the same work, however, τ was found to decrease rapidly as $\mu \rightarrow 0$. We speculate that this is related to the fact that at low μ most tangential forces will be fully mobilized so that the corresponding contacts are marginally close to slipping. This considerably decreases the number of force degrees of freedom, because the tangential force in a fully mobilized contact is fixed by the normal force and the value of μ [1]. These sheared systems at low μ are therefore less hyperstatic than one would naively think on the basis of the coordination number, and this significantly reduces their shear-resistance [19, 20]. However, for moderate μ contacts do not slip so easily and the packings become really hyperstatic (w.r.t. the frictional $z_{\text{iso}} = 3$) [26, 35]. Therefore, we expect the arguments put forward in this paper to be applicable in this regime.

The fact that the average force $\mathbf{f}(\phi)$ contains so much information about the stress state is due to the linearity of Eq. (2). The stress therefore only couples to the first moment of the force distributions, so we can ignore details of the extensively studied probability $P(|\mathbf{f}|)$ [3, 4, 5, 7, 8]. Also there the properties of the stress tensor do not require any “force chains”, i.e. the tendency of large forces to align in a correlated way. Eq. (2) does not invoke products of different \mathbf{f}_{ij} so that spatial force-force correlations do not come into play.

Another interesting perspective is that one can use $\mathbf{f}(\phi)$ to estimate the effective elastic moduli of the system, denoted by $C_{\alpha\beta\gamma\delta}$. It has been shown experimentally that these become highly anisotropic when a system is pre-sheared [6, 23]. The response to a localized vertical force on the free surface of a granular bed was found not to propagate along the vertical, but along a direction that is tilted towards the major stress axis. This indicates a stiffening of contacts along the major axis that are responsible for the anisotropic elasticity. By fitting the experimentally measured stress profiles Atman *et al.* [23] obtained the ratio $C_{1111}/C_{2222} \approx 0.67$ of the Young’s moduli in the minor (1) and major (2) directions. This finding was remarkably insensitive to frictional properties and roughness of the grains.

The stiffening of contacts can be explained through the nonlinear interaction between particles, which for frictionless Hertzian contacts [36] in three dimensions is $k_{ij} \propto f_{ij}^{1/3}$, where k_{ij} is the effective spring-constant of the contact. Assuming that the displacements of the particles are affine — this is reasonable for the strongly hyperstatic packings considered in this paper [37] — one can estimate the elastic moduli as [38, 39]

$$C_{\alpha\beta\gamma\delta} \propto \int_0^\pi d\phi \Phi(\phi) \bar{k}(\phi) n_\alpha n_\beta n_\gamma n_\delta$$

$$\propto \int_0^\pi d\phi \Phi(\phi) [\bar{f}(\phi)]^{1/3} n_\alpha n_\beta n_\gamma n_\delta. \quad (44)$$

This allows to systematically explore the effect of stress induced anisotropy in forces or fabric, by again using the Fourier expansions of $\bar{f}(\phi)$ and $\Phi(\phi)$. For the simplest case of isotropic frictionless contacts, one already finds that $C_{1111}/C_{2222} = 1 - 8\tau/9 + \mathcal{O}(\tau^2)$, so that the experimentally observed ratio of about 0.67 is easily achieved for realistic values of τ .

Acknowledgments

We thank M. van Hecke, T. Vlugt, J. Tailleur, P. Brunet, K. Shundyak, and W. van Saarloos for numerous discussions. WGE acknowledges financial support from the physics foundation FOM, JHS from a Marie Curie European Fellowship FP6 (MEIF-CT-2006-025104).

APPENDIX A: FRICTIONLESS CASE AT ARBITRARY ORDER

In this appendix we analytically solve the linear problem of Eq. (20). Due to the symmetry of $\bar{f}_n(\phi)$ we can write

$$\bar{f}_n(\phi) = 1 + \sum_{k=1}^N q_k \sin\left(2k\phi + \frac{(k-1)\pi}{2}\right). \quad (A1)$$

Comparing to Eq. (16), we find $q_k = (-1)^{(k-1)/2} a_k$ for odd k , while $q_k = (-1)^{k/2} b_k$ for even k . In particular, $q_1 = 2\tau$. The even derivatives can be written as

$$\frac{\partial^{2l}}{\partial \phi^{2l}} \bar{f}_n(\phi) = (-1)^l \sum_{k=1}^N q_k (2k)^{2l} \sin\left(2k\phi + \frac{(k-1)\pi}{2}\right), \quad (A2)$$

and since all sine terms evaluated at $\phi = 3\pi/4$ yield -1 , we find for $l \neq 0$

$$\left. \frac{\partial^{2l}}{\partial \phi^{2l}} \bar{f}_n(\phi) \right|_{\phi=3\pi/4} = (-1)^{l+1} \sum_{k=1}^N q_k (2k)^{2l}. \quad (A3)$$

The linear problem of Eq. (20) can now be written in the form of a Vandermonde matrix,

$$\begin{pmatrix} 1 & 1 & \dots & 1 \\ x_1 & x_2 & \dots & x_N \\ x_1^2 & x_2^2 & \dots & x_N^2 \\ \vdots & \vdots & \ddots & \vdots \\ x_1^{N-1} & x_2^{N-1} & \dots & x_N^{N-1} \end{pmatrix} \begin{pmatrix} q_1 \\ q_2 \\ q_3 \\ \vdots \\ q_N \end{pmatrix} = \begin{pmatrix} 1 \\ 0 \\ 0 \\ \vdots \\ 0 \end{pmatrix}, \quad (A4)$$

with $x_k = 4k^2$. The inverse A_{jk} of this matrix can be expressed explicitly in terms of Lagrange polynomials as [40]

$$P_j(x) = \prod_{k=1, k \neq j}^N \frac{x - x_k}{x_j - x_k} = \sum_{n=1}^N A_{jn} x^{n-1}. \quad (\text{A5})$$

We are interested in the solution for $q_1 = 2\tau$, which for Eq. (A4) simply reads

$$q_1 = A_{11} = P_1(0) = \prod_{k=2}^N \frac{x_k}{x_k - x_1}$$

$$= \prod_{k=2}^N \frac{k^2}{(k+1)(k-1)} = \frac{2N}{N+1}, \quad (\text{A6})$$

so that $\tau = N/(N+1)$, Eq. (21). Similarly, the other q_k follow from

$$q_k = \prod_{k=1, k \neq j}^N \frac{k^2}{(k+j)(k-j)}. \quad (\text{A7})$$

- [1] J.P. Bouchaud, in *Slow Relaxations and Nonequilibrium Dynamics in Condensed Matter*, Proceedings of the 2002 Les Houches Summer School, Session LXXVII (EDP Sciences, Les Ulis, 2003).
- [2] H.M. Jaeger, S.R. Nagel and R.P. Behringer, Rev. Mod. Phys. **68**, 1259 (1996); P.G. de Gennes, *ibid.* **71**, 374 (1999).
- [3] F. Radjai, M. Jean, J.J. Moreau and S. Roux, Phys. Rev. Lett. **77**, 274 (1996).
- [4] D.M. Mueth, H.M. Jaeger and S.R. Nagel, Phys. Rev. E **57**, 3164 (1998); D.L. Blair, N.W. Mueggenburg, A.H. Marshall, H.M. Jaeger, and S.R. Nagel, *ibid.* **63**, 041304 (2001).
- [5] J.H. Snoeijer, T.J.H. Vlugt, M. van Hecke and W. van Saarloos, Phys. Rev. Lett. **92**, 054302 (2004).
- [6] J. Geng, G. Reydellet, E. Clement, and R.P. Behringer, Physica D **182**, 274 (2003).
- [7] J. Brujic *et al.*, Faraday Discussions **123**, 207 (2003).
- [8] T.S. Majmudar and R.P. Behringer, Nature (London) **435**, 1079 (2005).
- [9] A.J. Liu and S.R. Nagel, Nature (London) **396**, 21 (1998).
- [10] A. Daerr and S. Douady, Nature (London) **399**, 241 (1999).
- [11] R.M. Nedderman, *Statics and Kinematics of Granular Materials* (Cambridge University Press, Cambridge, England 1992).
- [12] N. Xu and C.S. O'Hern, Phys. Rev. E **73**, 061303 (2006).
- [13] S. Nowak, A. Samadani and A. Kudrolli, Nature Physics (London) **1**, 50 (2005).
- [14] R. Albert, I. Albert, D. Hornbaker, P. Schiffer and A.L. Barabasi, Phys. Rev. E **56**, R6271 (1997).
- [15] F. Radjai and S. Roux, in *The Physics of Granular Media*, edited by H. Hinrichsen and D. E. Wolf (Wiley-VCH, Berlin, 2004), pp. 165.
- [16] F. da Cruz, S. Emam, M. Prochnow, J.-N. Roux, and F. Chevoir, Phys. Rev. E **72**, 021309 (2005).
- [17] S. Deboeuf, O. Dauchot, L. Staron, A. Mangeney, and J.-P. Vilotte, Phys. Rev. E **72**, 051305 (2005).
- [18] M. Oda, S. Nemat-Nasser, and J. Konishi, Soils and Foundations **25**, No. 3, 85 (1985).
- [19] G. Combe and J.N. Roux, Phys. Rev. Lett. **85**, 3628 (2000).
- [20] J.H. Snoeijer, W.G. Ellenbroek, T.J.H. Vlugt, and M. van Hecke, Phys. Rev. Lett. **96**, 098001 (2006).
- [21] I. Goldhirsch and C. Goldenberg, Eur. Phys. J. E **9**, 245 (2002).
- [22] F. Radjai, D.E. Wolf, M. Jean and J.J. Moreau, Phys. Rev. Lett. **80**, 61 (1998).
- [23] A.P.F. Atman *et al.*, Eur. Phys. J. E **17** 93 (2005).
- [24] C.F. Moukarzel, Phys. Rev. Lett. **81**, 1634 (1998).
- [25] A.V. Tkachenko and T.A. Witten, Phys. Rev. E **60**, 687 (1999).
- [26] T. Unger, J. Kertész, and D.E. Wolf, Phys. Rev. Lett. **94**, 178001 (2005).
- [27] B.P. Tighe, J.E.S. Socolar, D.G. Schaeffer, W.G. Mitchener and M.L. Huber, Phys. Rev. E **72**, 031306 (2005).
- [28] Actually, because for these values of the parameters the second derivative vanishes in $\phi = 3\pi/4$, we have to check that the fourth derivative is positive to be sure that the extremum is a minimum, which is indeed the case.
- [29] H. Troadec, F. Radjai, S. Roux, and J.C. Charmet, Phys. Rev. E **66**, 041305 (2002).
- [30] J. Jenkins, D. Johnson, L. La Ragione, and H. Makse, J. Mech. Phys. Solids **53**, 197 (2005).
- [31] See e.g. the *Coefficient of Friction* reference table on <http://www.engineershandbook.com/>
- [32] The maximum shear stress is achieved when contact and force anisotropy are “in phase”, so that we do not introduce a phase shift in the $\sin 2\phi$ term of Eq. (31).
- [33] F. Alonso-Marroquín, S. Luding, H.J. Herrmann, and I. Vardoulakis, Phys. Rev. E **71**, 051304 (2005).
- [34] A.P.F. Atman *et al.*, J. Phys.: Condens. Matter **17** S2391 (2005).
- [35] H.P. Zhang and H.A. Makse, Phys. Rev. E **72**, 011301 (2005).
- [36] K.L. Johnson, *Contact Mechanics* (Cambridge University Press, Cambridge, England, 1985).
- [37] W.G. Ellenbroek, E. Somfai, M. van Hecke, and W. van Saarloos, cond-mat/0604157.
- [38] K. Walton, J. Mech. Phys. Solids **35**, 213 (1987).
- [39] R.J. Bathurst and L. Rothenburg, J. Appl. Mech. **55**, 17 (1988).
- [40] W.H. Press *et al.*, in *Numerical Recipes in FORTRAN: The Art of Scientific Computing*, 2nd ed. (Cambridge University Press, Cambridge, England, 1992), pp. 82-89.